

# EFFECT OF LARGE DEFLECTIONS DURING IMPACT OF INFLATED THIN-WALLED SPHERICAL SHELL

W.J. Stronge  
University Of Cambridge  
Cambridge, UK, CB2 1PZ

A planar theory for oblique impact of an inflated thin-walled spherical shell (sports ball) against a rough rigid surface is presented and compared with rigid-body theory. This large deflection theory is based on assuming that during impact, the initially spherical ball flattens against the constraint surface while the remainder of the ball (moving with uniform translational velocity) remains undeformed. With the assumed deformation field, this theory for impact of a thin-walled shell includes a velocity discontinuity between the contact area that has been flattened and the moving part of the shell. During compression and restitution phases of contact, flow of momentum across the periphery of the flattened contact area results in a non-conservative momentum flux reaction. For a ball that is both translating and rotating, the distribution of the normal component of velocity for material entering and exiting the flattened contact area results in a distribution of momentum flux force intensity around the periphery of the contact region and consequently, a momentum flux torque acting on the flattened sphere. This paper relates changes in rebound velocity and rate-of-spin of thin-walled inflated spherical shells that result from impact to structural properties as well as the maximum deflection.

## 1. Introduction

For a thin-walled spherical shell (sports ball) colliding against a hard surface, a principal effect of the large deflections that develop during impact is a significantly large area of contact between the colliding bodies. As segments of the ball come into contact with the hard surface they are required to have a normal component of velocity that is compatible with that of the surface; i.e. in the contact area, the normal component of velocity must vanish. The distribution of velocity in the shell varies during the finite period of contact as the contact patch first increases and later decreases in size. For non-spinning thin-walled spherical shells with negligible flexural stiffness, Johnson et.al. [1] analysed changes in motion resulting from normal impact against a plane surface. They recognized that during impact, the part of the ball which is accelerating has variable mass and they used the term momentum flux force for that part of rate-of-change of momentum associated with transfer of mass from the

accelerating into the stationary part of the compressing sphere. Subsequently, Percival [2] corrected a perceived error in the previous analysis and explained why momentum flux force is irreversible.

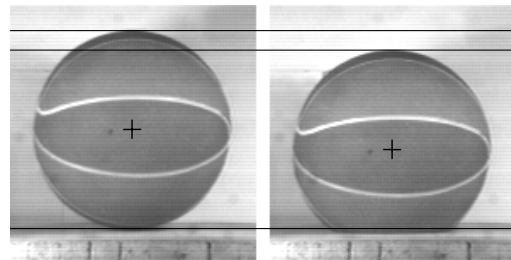


**Fig. 1:** High speed photographs showing maximum displacement,  $z_{max} = 0.2$ , resulting from a normal impact at  $6\text{ms}^{-1}$  of a size 5 basketball inflated to initial gauge pressure of 51kPa (8 psig).

Hubbard and Stronge [3] used a similar method to analyse sources of dissipation during impact of table tennis balls. The effect of rotation was added by Haake et.al. [4] who related momentum flux couple to the difference between the largest and smallest normal velocity across the contact patch. The present paper

differs from these previous investigations by considering the distributed reaction force acting at the periphery of the contact area where the change in momentum is occurring.

## 2. Properties of Deformed Thin-Walled Spherical Shell

Thin walled spherical shells which have large membrane stiffness but small flexural stiffness can be analysed by assuming that during impact, deformation occurs only in the contact region; i.e. an initially spherical cap is flattened against the contact surface. Outside the contact region, the remainder of the sphere is assumed to remain undeformed. With this kinematic assumption, the geometry of the deformed sphere can be expressed as a function of the indentation  $\delta$ , which is equal to the height of the

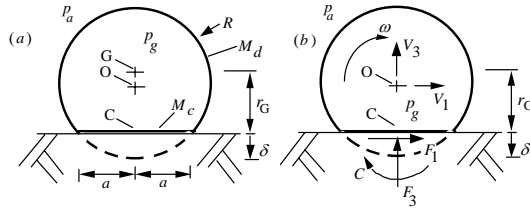


**Fig. 2.** a. Deformed configuration of inflated spherical shell and b. components of velocity  $V_i$ , angular velocity  $\omega$ , contact force  $F_i$  and contact couple  $C$ .

flattened cap in the initial, undeformed configuration, see Fig 2. For thin-walled shells, the contact radius  $a$  is related to initial radius  $R$  of the shell by

$$a/R = \sqrt{2\delta/R - \delta^2/R^2} \quad (1)$$

The flattened sphere has a center of mass  $G$  displaced a distance  $\varepsilon^2/R$  away from the center. Hence, there is distance  $r_G$  between the flattened cap and the center of mass  $G(\delta)$  of the

flattened spherical shell as shown in Fig 2.

$$r_G/R = (1 - \delta/2R)^2 \quad (2)$$

The initial mass  $M_0$  of a thin-walled spherical shell is  $M_0 = 4\pi\rho R^2 h$  where  $\rho$  is material density and  $h$  is wall thickness. A thin-walled spherical shell has mass distributed uniformly across the diameter so the mass of the flattened cap  $M_c$  is given by  $M_c/M_0 = \delta/2R$ .

Assuming that the flattened segment of sphere has only tangential velocity, the spherical segment of shell and flattened cap have moment of inertia  $I_G$  about the center of mass  $G(\delta)$ . The ratio of moment-of-inertia of the deformed sphere  $I_G$  to moment-of-inertia of the undeformed thin-walled sphere  $I_0 = (2/3)M_0R^2$  is

$$\frac{I_G}{I_0} = \left( 1 - \frac{9}{8} \frac{\delta^2}{R^2} + \frac{15}{24} \frac{\delta^3}{R^3} - \frac{3}{32} \frac{\delta^4}{R^4} \right) \quad (3)$$

A gas pressurized, thin-walled shell has an initial volume  $V_0 = (4/3)\pi R^3$  which is decreased by volume  $V_c$  of the spherical cap,  $V_c/V_0 = (\delta^2/4R^2)(3 - \delta/R)$ . Thus at any deflection  $\delta$ , the internal volume of a thin-walled sphere decreases to  $V(\delta) = V_0 - V_c$ . The pressure – volume relation for a perfect gas then gives the ratio of internal pressure  $p_g(\delta)$  to atmospheric pressure  $p_a$  outside the shell as

$$\begin{aligned} \frac{p_g}{p_a} &= \left( \frac{V(\delta)}{V_0} \right)^{-\gamma} \\ &= \frac{p_g(0)}{p_a} \left[ 1 - \frac{1}{4} \frac{\delta^2}{R^2} \left( 3 - \frac{\delta}{R} \right) \right]^{-\gamma} \quad (4) \end{aligned}$$

where specific heat ratio for air,  $\gamma = 1.4$  and initial internal pressure,  $p_0 = p_g(0)$ .

### 3. Normal Force at Contact Surface

#### 3.1 Gas Force Acting on Contact Area

As inertia presses a colliding thin-walled spherical ball against a flat surface, a contact force develops — this both deforms the shell and compresses the gas within the shell. If the shell is thin-walled and it has a relatively small elastic modulus — e.g. a rubber ball — the flexural stiffness of the shell is negligible so the normal force arises almost solely from internal pressure in the ball pressing the contact area of the shell against the contact surface. This gas force  $F_g = \pi a^2(p_g(\delta) - p_a)$  depends on the difference between the current internal gas pressure  $p_g(\delta)$  and atmospheric pressure  $p_a$ . This force increases with increasing contact area,  $F_g = \pi a^2(p_g(\delta) - p_a)$ . Internal pressure changes with deflection  $\delta/R$  in accord with expressions (3) and (4); hence,

$$\frac{F_g}{\pi R^2 p_a} = \left( \frac{2\delta}{R} - \frac{\delta^2}{R^2} \right) \times \left\{ -1 + \frac{p_g(0)}{p_a} \left[ 1 - \frac{1}{4} \frac{\delta^2}{R^2} \left( 3 - \frac{\delta}{R} \right) \right]^{-\gamma} \right\} \quad (5)$$

#### 3.2 Momentum Flux Force and Couple

As material flows across the interface into the deformed cap during approach or compression, at the contact surface a momentum flux force decelerates the inflowing

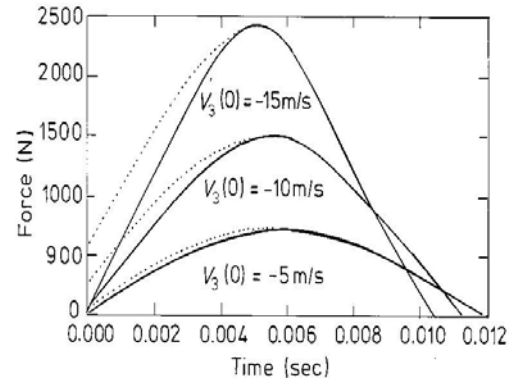


**Fig. 3.** Normal force during bounce of basketball (size 7) with  $p_g(0) = 152\text{kPa}$  or 8psig. Dotted line includes momentum flux. Speeds give max. deflection  $\delta_{\max}/R = 0.15, 0.30$  &  $0.43$ .

material from an incoming velocity equal to that of the shell, to the velocity of the cap (i.e.  $V_3 = 0$ ). This dynamic force results from transfer and subsequent deceleration of momentum across the interface between the moving spherical segment of shell and the flattened cap. Across this interface the momentum flux force intensity varies around the contact circle, depending on the local normal component of relative velocity  $V_3 - a\omega \cos \theta$  where  $V_3$  is normal velocity,  $\omega$  is angular velocity of the truncated spherical shell and  $\theta$  is angular position of an element of the contact circle measured from the tangential direction of motion  $n_1$ , (see Fig 2). Consequently, this analysis separates the period of collision into 3 distinct periods: (a) a period of compression where the entire periphery of the contact circle is being compressed, (b) a period of transition where one side of the contact circle is being compressed and the other is separating, and (c) a period of restitution when the spherical segment of shell is separating from the contact surface. Integration of force

intensity gives the momentum flux force  $F_{mf}$  and couple  $C_{mf}$  obtained by Stronge and Ashcroft [5].

$$F_{mf} = \frac{2}{2\pi} \int_0^{\theta_T} \frac{dM_c}{d\delta} V_3 [V_3 - a\omega \cos \theta] d\theta \quad (6)$$

$$C_{mf} = \frac{2}{2\pi} \int_0^{\theta_T} \frac{dM_c}{d\delta} V_3 \times [V_3 - a\omega \cos \theta] a \cos \theta d\theta \quad (7)$$

where the angular region of compression  $0 - \theta_T$  is given by,

$$\theta_T = \begin{cases} \pi & V_3 / a\omega < -1 \\ \cos^{-1}(V_3 / a\omega) & -1 < V_3 / a\omega < +1 \\ 0 & +1 < V_3 / a\omega \end{cases}$$

As shown in Fig. 3, the moment flux force and couple act during the period of compression only.

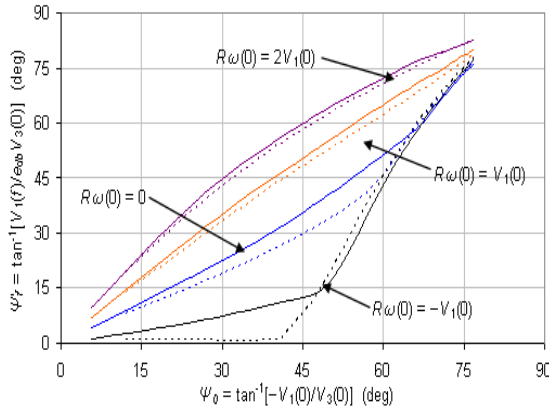


**Fig. 4.** Rigid body (cont. curve) and large deflection (dotted curve) calculations of angle of rebound as function of angle of incidence for basketball (size 7, initial press.  $p_g(0) = 152\text{kPa}$ ).

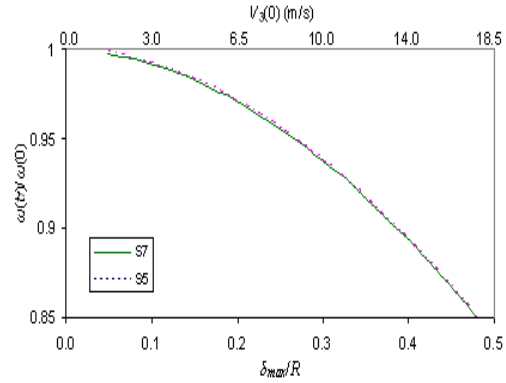


**Fig. 5.** Momentum flux couple gives decrease in ratio of final to initial angular velocity  $\omega(t_f)/\omega(0)$  of basketball (both size 5 & 7) with increasing max. displ.  $\delta_{\max}/R$  or impact velocity  $V_3(0)$  during frictionless impact,  $\mu = 0$ .

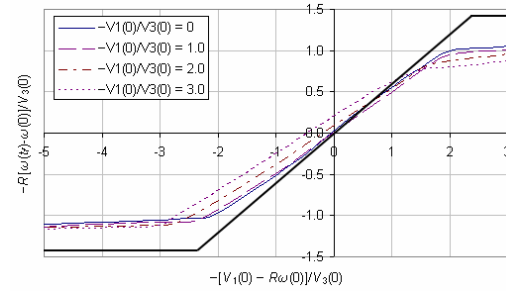


**Fig. 6.** Change in angular velocity as a function of the initial sliding velocity at contact point for initial normal impact speed  $V_3(0) = -18.5\text{m/s}$  ( $z_{\max} = 0.5$ )

#### 4. Conclusion

For maximum deflections as large as 1/3 the initial radius, the effect of finite deflections on the bounce of an inflated thin-walled spherical shell is surprisingly small – the angle of bounce is within 5% of the value obtained from rigid-body theory (Fig. 4) and the angular velocity or spin is decreased by 8% due to the momentum flux torque (Fig. 6). At this deflection,

hysteresis of the momentum flux force accounts for roughly a 20% decrease in kinetic energy of normal relative motion.

## 5. References

1. Johnson W, Reid SR, and Trembaczowski-Ryder RE. (1972) Impact, rebound and flight of a well-inflated pellicle as exemplified in association football. *Manchester Assoc Engineers* 5:1-25.
2. Percival A. (1976) The impact and rebound of a football. *Manchester Assoc Eng* 5:17-29.
3. Hubbard, M. and Stronge, W.J. (2001) Bounce of Hollow Balls on Flat Surfaces. *Int'l J Sports Engineering*, 4(2), 49-61.
4. Haake, S.J., Carre, M. and Goodwill, S. (2003) Modelling of oblique tennis ball impacts on tennis surfaces, *Tennis Science and Technology* 2 (ed. S. Miller) ITF London, 133-137.
5. Stronge, W.J. and A. Ashcroft (2007) Oblique impact of inflated balls at large deflection. *Int'l J. Impact Engineering* 34, 1003-1019.

